

Short Term Coastal Changes Along Damietta-Port Said Coast Northeast of the Nile Delta, Egypt

Hesham M. El-Asmar

Department of Geology
Damietta Faculty of Science
Damietta-34517, Egypt

ABSTRACT

EL-ASMAR, H.M., 2002. Short term coastal changes along Damietta-Port Said coast northeast of the Nile Delta, Egypt. *Journal of Coastal Research*, 18(3), 433–441. West Palm Beach (Florida), ISSN 0749-0208.



Landsat Thematic Mapper images (TM) covered the coastline between Damietta and Port Said, taken at intervals in 1984, 1987 and 1991, were used to detect shoreline changes. When combined with geomorphological and sedimentological data, the remote sensing data enable the classification of the coastline into five segments, based on whether erosional or depositional process domains dominate them. Although the 30m spatial resolution of the satellite TM data precludes precise calculation of rates of change, they do enable erosional and accretionary coastline segments of the Damietta Port Said coast to be recognised over these time scales. Segments 1 and 2 are erosional with an average shoreline recession of -41.4 m yr^{-1} , and -19.3 m yr^{-1} respectively. Segment 3, Damietta spit, is an accretionary segment with an average shoreline advance of 81.4 m yr^{-1} . Segment 4, El-Deiba, experienced erosion in the period 1984–1987, with an average shoreline recession of -17 m yr^{-1} , but appears to have been stable over most of its length during the period 1987–1991, with observed declaration in the rate of shoreline recession to be -2.5 m yr^{-1} . Segment 5, El-Gamiel, was stable during the period 1984–1987, but due to the construction of projecting jetties around the mouth of the inlet and the subsequent interruption of the sediment transport supply, the coastline became accretionary updrift of the inlet (west) and erosional downdrift (east). Granulometric and heavy mineral analyses show significant differences between beach face sediment samples collected from the different coastline segments. The erosional segments are characterised by coarser sands and high concentrations of heavy minerals; while the accretionary segments are composed of finer sands with lower concentrations of heavy minerals. Poor coastal management strategies and the shortage of data on geomorphological processes along the coast has resulted in constructions taking place along sections of erosional coastline, requiring subsequent expensive defence measures. Moreover, these results have implication for future development on onshore facilities after the recent discovery of oil and gas reserves offshore.

ADDITIONAL INDEX WORDS: Nile Delta, coastline, erosion, Damietta, Port Said, satellite images.

INTRODUCTION

The Nile Delta is a classic landform, the word delta is derived from the Greek character Δ , the shape of which the Nile delta resembles in plan form (SESTINI, 1989). The Nile Delta coastline consists of sandy arcuate beaches creating a fully dissipative wave environment for most of its length, backed by coastal flats, dunes and lagoons (NAFAA and FRIHY, 1993). Long term monitoring of shoreline changes along the Nile Delta coastline using ancient maps has demonstrated a progradation of some 3–4 km during the 19th century, followed by erosion and shoreline retreat of some 106 m yr^{-1} during the period 1970–1990 (LOTFY and FRIHY, 1993; FRIHY and KOMAR, 1993). This is attributed mostly to the reduction in supply of fluvial sediments from the Nile consequent to construction of the hydrological control structures, chiefly the Aswan High Dam completed in 1964. Sediment entrapment along the 10,000 km of artificial canals in the delta, climate changes in East Africa, land subsidence and sea level rise, have also been implicated by various workers (FOUCAULT and STANLEY, 1989; EL-ASMAR, 1994 and 1995; STANLEY and WINGERATH, 1996).

Seasonal wave climatology data along Ras El-Bar and Port

Said were given in SHARAF EL-DIN and MAHAR (1997), and summarized in Table (1). Due to the effect of the prevailing NNW-N and WNW-NNW stormy winter waves at Ras El-Bar and Port Said respectively, the longshore current is found to be eastward, with a small westward component resulted from the effect of the NNE swells during spring and summer. The direction and velocity of the littoral current were measured along the eastern (present study area) and the western (Ras El-Bar) coastline of the Damietta mouth during the periods from January to December 1991 and from January to July 1993 (BADR and LOTFY, 1998 and 1999). At the west of the Damietta mouth the percentage of the occurrence of the eastward current ranges between 65% and 83%, with a mean velocity of 44.48 cm s^{-1} , while westward current ranges from 15% to 20%, with a mean velocity of $30\text{--}34 \text{ cm s}^{-1}$. On the other hand, the measurements at the east of the Damietta mouth show eastward current ranges between 84% and 89%, with a mean velocity of $41\text{--}47 \text{ cm s}^{-1}$, while the westward current ranges between 10–12%, with a mean velocity of $33\text{--}36 \text{ cm s}^{-1}$. The Mediterranean Sea at the Nile Delta is virtually tideless, the tide gauge at Burullus inlet showed a tidal range of only 14 cm in the 20 years (EL-FISHAWI, 1994), with 60 cm variation in daily mean sea level at Port Said (EID *et al.*, 1997).

Table 1. Wave climatology along Damietta-Port Said coastline.

Damietta				
Wave Height $\leq 2\text{m}$	19.4%	11.9%	2.5%	6.8%
Wave Direction	80% NNW-N	94% NNW-N	85% NNW-N	99% NNW-NNE
Port Said				
Wave Height $\leq 2\text{m}$	18%	6.1%	2.7%	7.5%
Wave Direction	75% NNW-N	72% NW-NNW	70% NW-NNW	47% N-NNE
Wave Period	4.8s-9s	4.4s-7.6s	4.1s-7.7s	4.6s-9.3s

This paper combines satellite remote sensing data with conventional geomorphological and sedimentological data, including grain size and heavy mineral analyses to examine the distribution of processes domain along the section of the coast from Damietta to Port Said. This coast is experiencing considerable development pressure at present, and looks set to increase after the recent discovery of offshore oil and gas reserves.

METHODOLOGY

Remote sensing has been widely used to monitor coastal changes along the Nile Delta coastline; however, most studies have focused on the long term and on areas of very rapid changes such as the Rosetta promontory. By applying advanced pattern recognition algorithms to Landsat Thematic Mapper images, EL-ASMAR and WHITE (1997) were able to automate the process of extraction of coastline from the data and monitor coastal changes over the whole Nile Delta. They demonstrated that these data can be used to detect changes during the short timescale of 1984–1987–1991.

Landsat Thematic Mapper data were acquired covering the Nile Delta coastline from Damietta to Port Said (path 176 row 38—Worldwide reference system) for three dates (1984, 1987 and 1990/91). The 1991 scene was registered to geographical coordinates using a second order polynomial to transform the line and column locations of pixels to their latitude and longitude locations, derived from map and G.P.S. data. The root mean square (R.M.S.) error is also calculated for each ground control point (G.C.P.), to provide a measure of the residuals associated with the transformation. The lower the R.M.S. error, the better the fit of the transformation to the G.C.P.'s. In this project, no single G.C.P. was permitted to have a R.M.S. error greater than 1 pixel (or 0.5 pixel for image-to-image registration, where G.C.P.'s can be more accurately located). The mean R.M.S. error for all the G.C.P.'s was not permitted to exceed 0.55 pixel (or 0.4 pixel for image-to-image registration). A full analysis of the geographical accuracy of the image products used in this project is given elsewhere (WHITE and EL-ASMAR, 1999).

In order to delineate the coastline, Thematic Mapper band 7 (shortwave infrared) was used. Shorter wavelengths allow some penetration through water, giving amore gradational effect and making exact delineation of the coastline difficult (WILSON, 1997). The shortwave infrared data also reduces the impact of high-reflectance surf in the breaker zone (FROUIN *et al.*, 1996).

Image segmentation and edge detection algorithms, developed for robot vision, follow the process of human image in-

terpretation (CROSS *et al.*, 1988), by dividing an image into different regions (SONKA *et al.*, 1993). There are two techniques, the edge detection (disjunctive) approach finds and links high frequency edges around regions by passing spatial convolution filters over the image. The alternative (conjunctive) approach seeks to grow homogeneous regions by merging pixels or sub-regions on the basis of some similarity criterion (LEMOIGNE and TILTON, 1995). The latter, region-growing, approach has been found to be more suitable for most remote sensing applications (KETTIG and LANDGREBE, 1976) and is adopted here. The segmentation of different land cover types, such as agricultural land use, various measurements of texture are normally necessary (WESZKA *et al.*, 1976; CHEN and PAVLIDIS, 1979). Segmentation of land and water in shortwave infrared optical images can usually be implemented using a specified grey level difference from the region mean as a homogeneity criterion, by virtue of their distinct spectral reflectance characteristics at these wavelengths. In this project, mean and standard deviation statistics of beach surfaces and water surfaces were extracted from the georeferenced imagery and used to specify the homogeneity criterion.

Little pre-processing is necessary for automatic segmentation of water (WILSON, 1997). In order to ensure that the same homogeneity criterion could be applied to all images, a cosine correction was applied for differences in sun angle arising from the different times of the year that the images were collected. This only had a minimal effect on DN values, as all images were acquired in the Northern Hemisphere summer months between May and August. A DN difference from region mean of 20 was found to account for variability in the sea reflectance in TM band 7, while still ensuring that the coast was always picked up as a region boundary. The region mean was updated with each additional merge. Region growing was initiated at the same point over the sea for each date, in order to avoid differences arising from merging order. Cloud regions over the sea were deleted and interior shorelines of the Manzala lagoon, picked up as the region growth extended down canals and drainage channels, were deleted manually to leave only the coastline. The resulting vectors are located at intercell, rather than on-cell boundaries (FLECK, 1992), forming a crack-edge representation of the coastline of the Nile Delta at the time of image acquisition.

Sediment characteristics can also be used to recognise the dominant processes domain at a location on a coastline. Samples of beach-face sediments were collected at numerous points along the shoreline under consideration. Three samples were collected at each sample location, one at the low

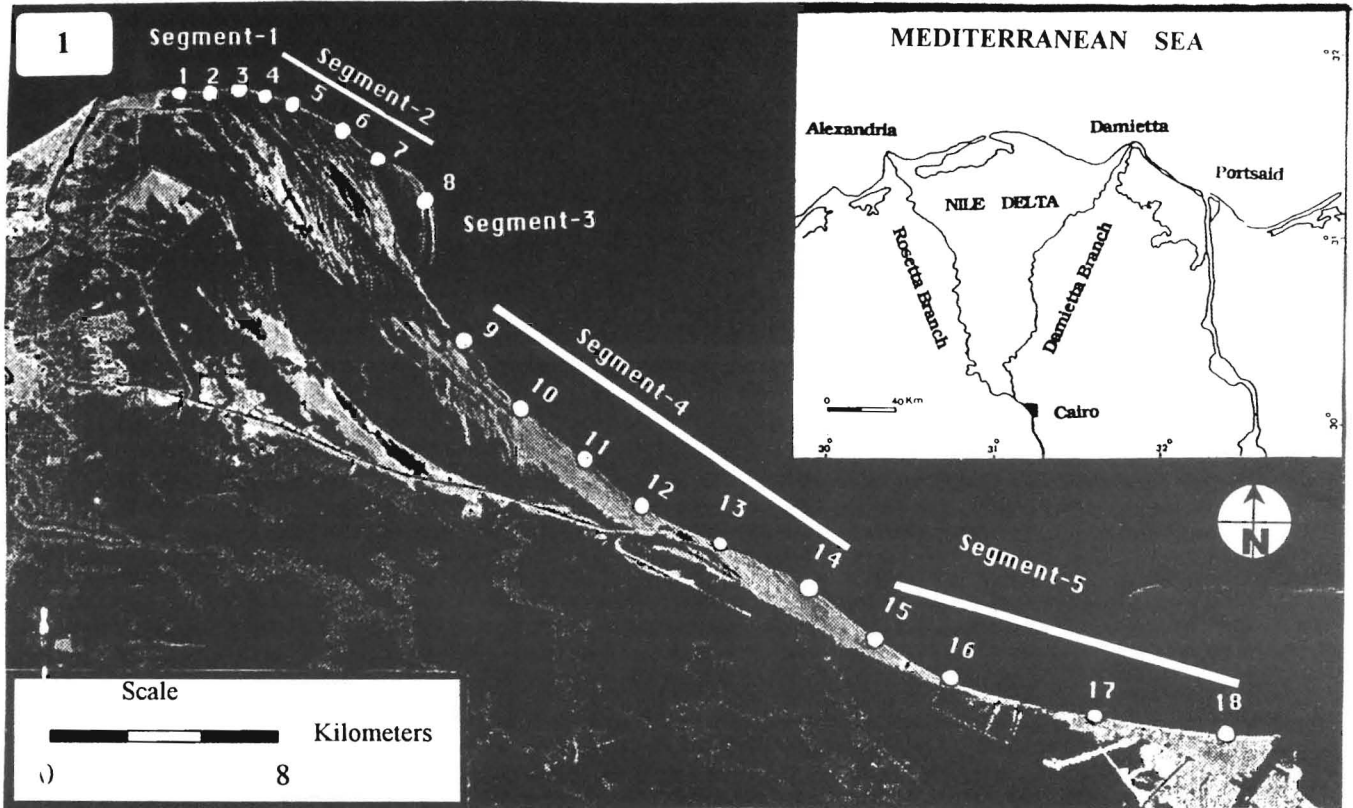


Figure 1. Location map and coastline segments along the Damietta and Port Said, northeast of the Nile Delta, Egypt.

Table 2. Shoreline changes along the coastline between the Damietta and Port Said, northeast of the Nile Delta, Egypt, deduced from the Thematic Mapper Imagery of 1984, 1987 and 1991.

Measurement sites	Shoreline Changes* 1984–1987 (m yr ⁻¹)		Shoreline Changes 1987–1991 (m yr ⁻¹)		Total Changes 1984– 1991 (m yr ⁻¹)	
	Measured	Average	Measured	Average	Measured	Average
SEGMENT-1	1	-90	-150		-240	
	2	-180	-43	-150	-330	-41.4
	3	-120		-180	-300	
SEGMENT-2	4	-60	-90		-150	
	5	-60	-20	-90	-150	-19.3
	6	-60		-30	-90	
	7	-60		-90	-150	
SEGMENT-3	8	270	90	300	570	81.4
SEGMENT-4	9	-60		-90	-150	
	10	-90		-60	-150	
	11	-30	-17	60	30	-8.6
	12	-30		60	30	
	13	-30		-30	-60	
SEGMENT-5	14	-60		0	-60	
	15	0		30	30	
	16	60	5	-30	30	2.1
	17	0		0	0	
	18	0		0	0	

* Figures are in meter, measurements are taken normal to the shoreline and quantified to 30m pixel interval. Negative values indicate shoreline recession, while the positive ones indicate accretion.

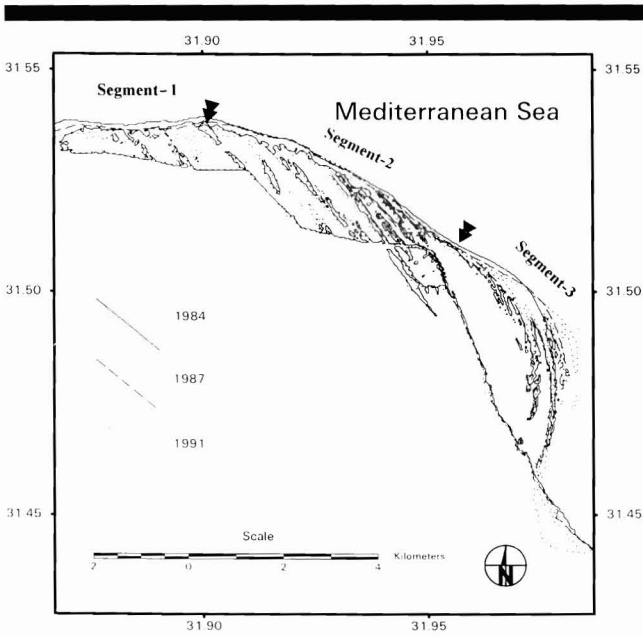


Figure 2. Vector map showing shoreline changes along the coastline segments 1, 2 and 3 east of Damietta mouth and Damietta spit, deduced from the Satellite Thematic Mapper Imagery of 1984, 1987 and 1991.

water mark, one at the high water mark, and one in the middle. These were wet-sieved into phi particle size classes and the weights of these classes were used to determine the particle size distribution. Total heavy mineral content was determined for the fine sand fraction of all samples.

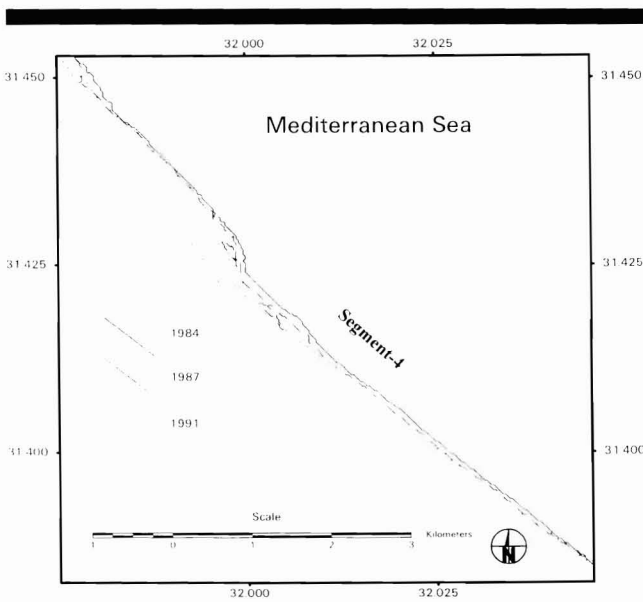


Figure 3. Vector map showing shoreline changes along the coastline segment-4 (El-Deiba), deduced from the Satellite Thematic Mapper Imagery of 1984, 1987 and 1991.

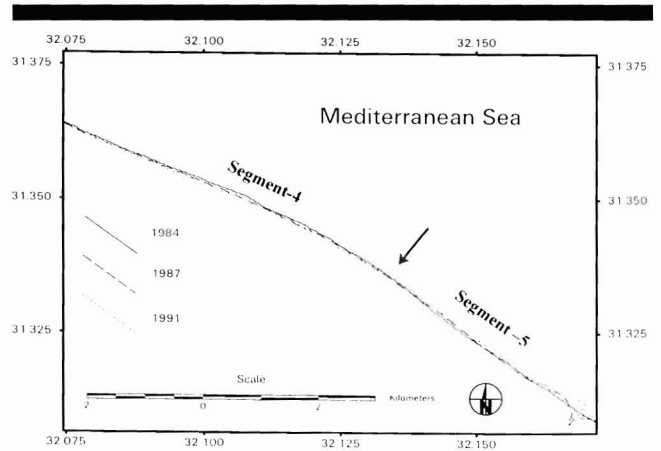


Figure 4. Vector map showing shoreline changes and the nodal point (arrow) between the erosional coastline segment-4 (El-Deiba) and the accretional coastline segment-5 (El-Gamiel), deduced from the Satellite Thematic Mapper Imagery of 1984, 1987 and 1991.

RESULTS AND DISCUSSION

18 monitoring points were selected along the coastline between Damietta and Port Said (Figure 1). At these points, shoreline positions have been monitored from the satellite imagery and measurements (in units of 1 pixel = 30 m) of the movement in the periods 1984–1987 and 1987–1991 were made (Table 2). On the basis of these measurements, and the orientation of the coastline, the shoreline is subdivided into five segments based on whether erosional or depositional process domains are dominant. Points 1–7 are within segments 1 and 2 (Figure 1), which lie immediately adjacent to the

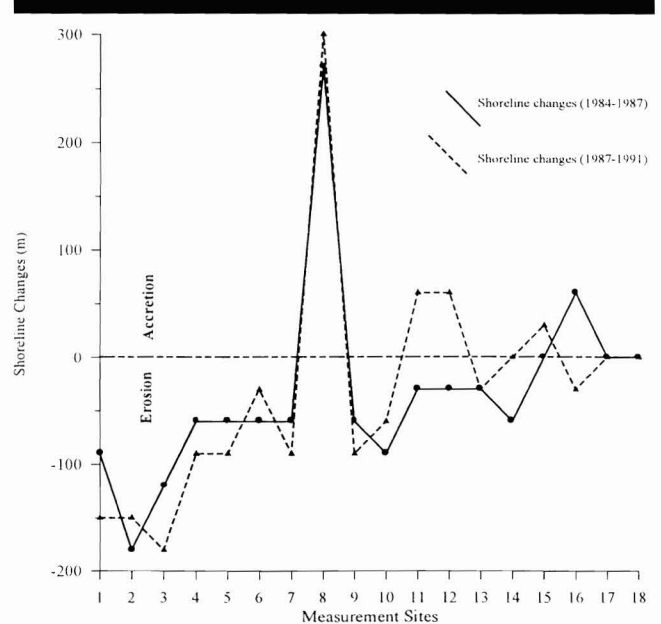


Figure 5. Shoreline changes along the coastline between Damietta and Port Said during the periods 1984–1987 and 1987–1991.

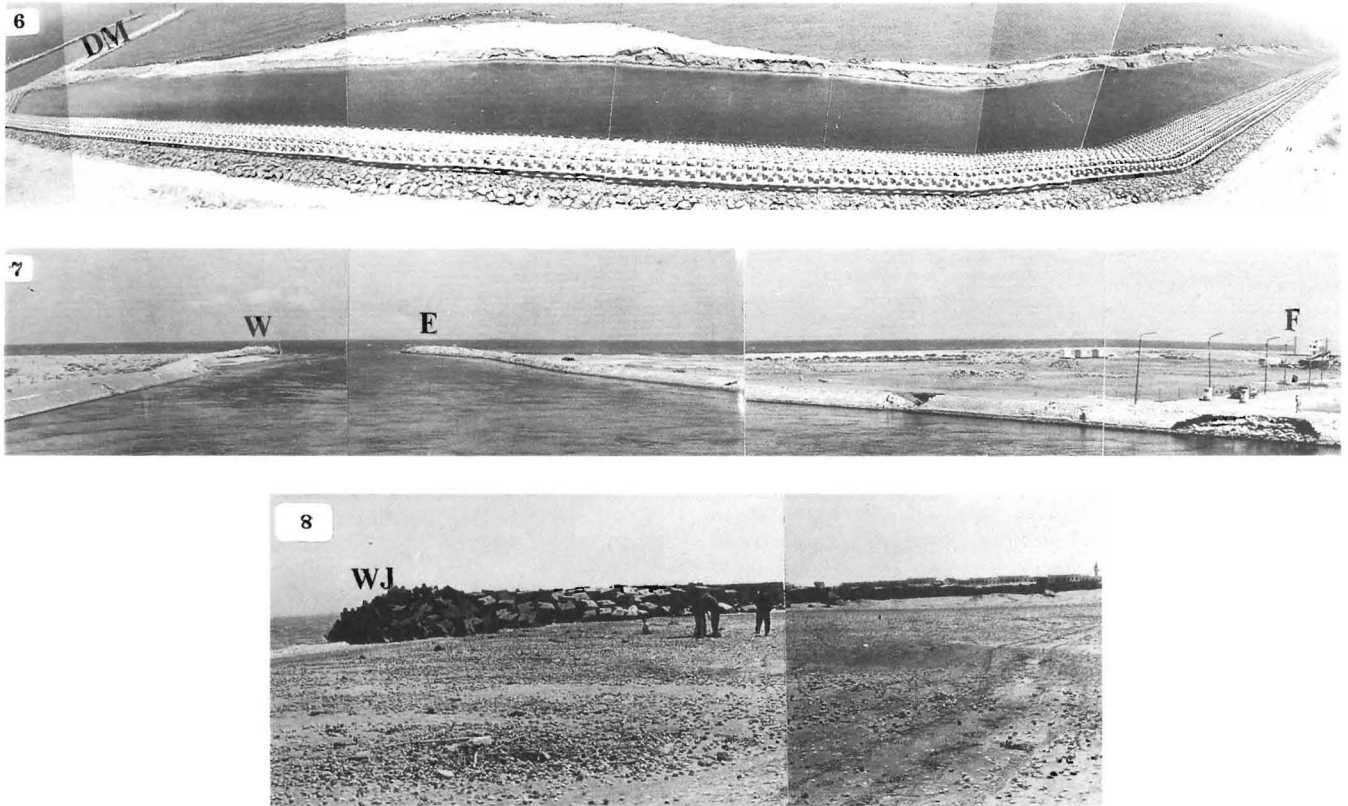


Figure 6. The recently constructed seawall (revetment) along the coastline east of the Damietta mouth "DM" for a distance of about 5km to protect segments 1, and 2 from erosion.

Figure 7. Two jetties "W, E" constructed to prevent sedimentation of drifted sands along El-Gamiel inlet from El-Fardows tourist village "F" appears at the extreme right-side of the photo, constructed at the erosional down-drift side of the inlet.

Figure 8. Sedimentation at the up-drift western jetty "WJ" of El-Gamiel inlet.

mouth of the Damietta branch of the Nile, are experiencing rapid rates of erosion and shoreline recession (Figures 2, 5; Table 2) with the barrier beach migrating back over the Manzala lagoon. The average shoreline recession along segment-1 during the period 1984 to 1991 is -41.4 m yr^{-1} , while the average recession along segment-2 is -19.3 m yr^{-1} (Table 2). Importance of coastline orientation is evident from these data; segment-1 has an ENE-WSW trend and has experienced much greater amounts of erosion than segment-2, which has a NW-SE trend (Figure 2). Eastward moving long-shore currents set up by waves approaching the coast from the NW-NNW feed the spit platform. When waves approach from an opposite oblique quadrant (NNE) the spit platform undergoes erosion, which was evidenced elsewhere by Friedman *et al.* (1992).

Long term erosion rates along this section of coastline has been estimated from historical maps to be in the range of -35 to -50 m yr^{-1} between 1945–1973 (SESTINI, 1992). SMITH and ABDELKADER (1988) determined a rate of -50 to -60 m yr^{-1} for the period 1973–1984. FRIHY and KOMAR (1993) determined an erosion rate of -10 m yr^{-1} for the period 1971–1990. More recently, ABOU EL-MAGD (1995) has suggested

an erosion rate of -37 m yr^{-1} , focused at a point coinciding with sampling points 2 and 3 (Figure 1). Rates of -9.8 m yr^{-1} and -44 m yr^{-1} was suggested during the period 1922–1995 (FRIHY *et al.*, 1998a and b). The discrepancy in Frihy's rates came from using wide range time interval, including the period 1922–1964 before the construction of Aswan High Dam, during which no erosion was detected along the Damietta Promontory.

The beach sand transport and the littoral drift along the coastline east of the Damietta mouth were studied using heavy mineral distribution and fluorescent sand tracers (EL-ASKARY and BADR, 1996; BADR and LOTFY, 1998 and 1999). Accordingly, the severe erosion along this coastline was interpreted as being due to the higher grain velocity and the thicker mobile bed layer. These studies have demonstrated that the average depletion rate was 39.4×10^6 and $41.65 \times 10^6 \text{ grain min}^{-1}$ during 1991 and 1993 respectively. The grain velocity ranges from 3.07 – 3.51 m min^{-1} and thickness of mobile layer of 2.0 to 3.0 cm . Thus, the annual drift rate has estimated to be between 2.21×10^6 to $3.19 \times 10^6 \text{ m}^3 \text{ yr}^{-1}$.

Point 8 is located at the eastern end of the contemporary spit (Figure 1), represented by an accretionary segment (seg-

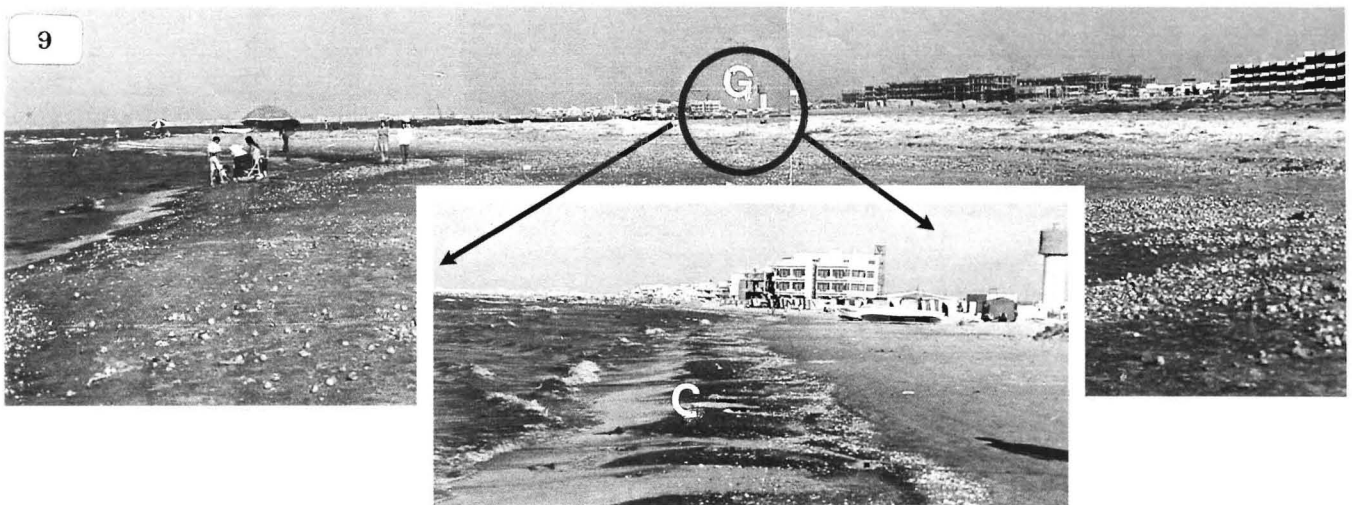


Figure 9. Erosional features including the cusped beach "C" and shall accumulations along the coastline east of El-Gamiel inlet at the tourist village "G".

Figure 10. Sedimentation "S" at the western jetty of El-Gamiel inlet due to sediments delivered by NE summer waves.

ment-3) where the shoreline is advancing at a rate of 81.4 m yr^{-1} (Table 2, Figures 2 and 5), fed by material eroded from segments 1 and 2. A rate of 75 m yr^{-1} was suggested by ABOU EL-MAGD (1995). The contemporary spit formed in 1955 and has subsequently migrated laterally to the SE (MANOHAR, 1981). This has taken place under the sediment transport flux set up by the NW-NNW wave direction, reaching 5–6 km length during 1971–1975 (HAMAMA, 1978; LOTFY, 1978), and 10 km length by 1991 (Figure 2). FRIHY *et al.* (1998b) have suggested a lengthening rate of 170 m yr^{-1} and an increasing in the width by 60 m yr^{-1} , with shoreline accretion of 8 m yr^{-1} . Recently, a seawall (Figure 6) has been constructed along 5 km of the coastline (segment-1, Figure 1). While this will control erosion in segment-1, it will starve the spit sediment and ultimately lead to erosion of segment-3.

Points 9–14 lie within segment-4 (El-Deiba, Figures 1 and 3). During 1984–1987, it experienced significant erosion with

an average shoreline recession of -17 m yr^{-1} (Table 1; Figure 5). During the period 1987–1991 this segment subsequently became more stable and deceleration in the rate of shoreline recession is observed (Table 1; Figure 5). The detected average shoreline recession was -2.5 m yr^{-1} , with some points (9, 10 and 13; Table 2) experiencing erosion, and others (points 11 and 12; Table 2) experience accretion (Figure 5). Rates of erosion of -7 to -16 m yr^{-1} have been estimated from conventional surveys of this segment of the coast (ABOU EL-MAGD, 1995; SMITH and ABDELKADER, 1988).

Points 15–18 lie within segment-5 (El-Gamiel. Figures 1 and 4). This segment of coastline was stable between 1984–1987, but experienced some accretion in some places. A rate of shoreline advance of 5 m yr^{-1} is here adopted (Table 2; Figures 4 and 5), and a volumetric sand accretion of $2.6 \times 10^6 \text{ m}^3$ was measured during the period 1978–1981 (LOTFY and FRIHY, 1993). However, at some stages within the period

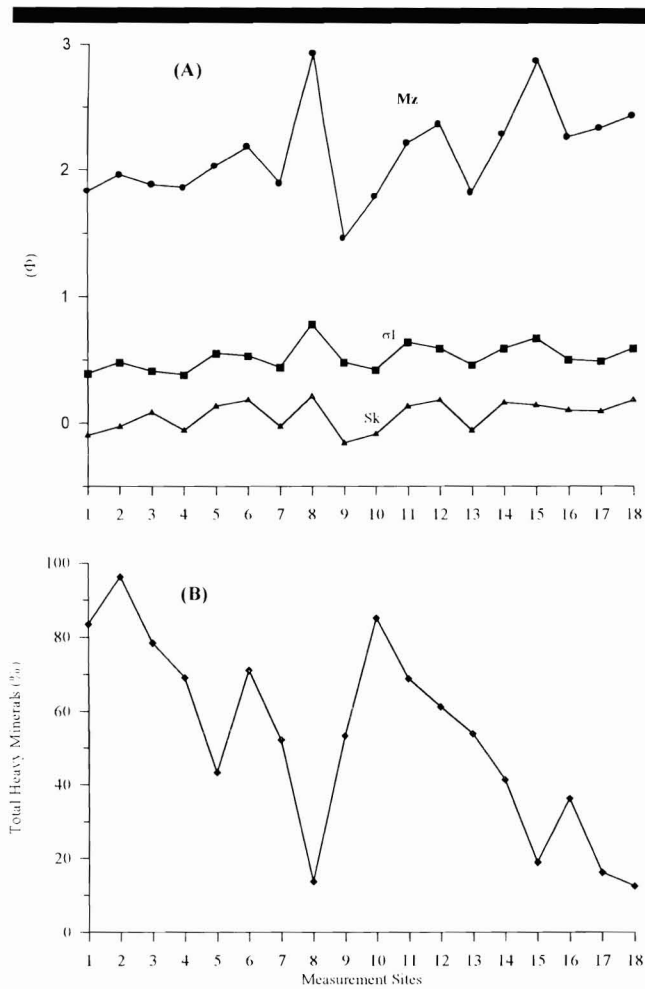


Figure 11. Distributions of grain size parameters (A) and total heavy minerals (B) at the studied sites along the Damietta and Port Said coast, northeast of the Nile Delta.

1987–1991, an artificial inlet to the Manzala lagoon was constructed at El-Gamiel to improve the water circulation in the lagoon. Two jetties were constructed on either sides of the inlet to protect it from siltup by the longshore sediment flux (Figure 7). However, the jetties have created a discontinuity in the eastward-moving longshore flux, resulting in accretion against the western jetty (Figure 8) and erosion (Figure 9) adjacent to the eastern jetty (Table 2; points 15 and 16). Despite the jetty construction, the channel is experiencing significant siltation from the longshore drift, and from the delivery of sediment by the summer NE wave direction (Figure 10). Clearly mechanical dredging will be required at some future date.

The sediment samples demonstrate significant differences between the erosional and accretionary coastline segments recognised from the remote sensing TM images. Erosional segments are characterised by coarser sands with high heavy mineral (H. M.) content (Table 3; Figure 11), while accretionary segments are characterised by finer sands with lower (H. M.) content (Table 3, Figure 11). For example, the erosional segments 1, 2 and 4 have a mean phi particle size of 1.97 Φ (medium sands), well sorted ($\sigma = 0.44 \Phi$), near symmetrical ($Sk = 0.03 \Phi$), and have a mean (H. M.) content of 65.88% by weight of fine sand. The accretional segments 3 and 5 have a mean phi particle size of 2.56 Φ (fine sands), moderately well sorted ($\sigma = 0.61\Phi$), and skewed to the finer fraction ($Sk = 0.14 \Phi$), with a mean (H. M.) content of 19.4% by weight of fine sands (Table 3, Fig. 11).

The frequency distribution of grain size parameters and total heavy mineral (T.H.M.) concentrations along the Damietta coast show that most of the sediments belong to fine sands and display a mode between 1–3 Φ (EL-ASKARY and LOTFY, 1995). The average well-sorted sands are in the range of 77.08% with near symmetrical distribution and only 6.25% of the distribution show negative skewness (EL-ASKARY and BADR, 1996). The encountered total heavy mineral (T.H.M.) percent along the Damietta coast is 13.74%, with higher concentrations recorded at the eroded sands, range from 3.4% to 89.8% with an average of 37.17%. The accreted sands, on the

Table 3. Sedimentological characteristics and total heavy mineral distributions along the Damietta-Port Said coast, northeast of the Nile Delta, Egypt.

Measurement Sites and Characters			Mz(ϕ)	σ (ϕ)	Sk(ϕ)	(T.H.M.) %	
SEGMENT-1	East Damietta spit	Erosional	1	1.83	0.39	-0.10	83.40
			2	1.96	0.48	-0.03	96.30
			3	1.88	0.41	0.08	78.38
SEGMENT-2	East Damietta spit	Erosional	4	1.86	0.38	-0.06	68.96
			5	2.03	0.55	0.13	43.16
			6	2.18	0.53	0.18	71.03
7	1.89	0.44	-0.03	52.11			
SEGMENT-3	Damietta spit	Depositional	8	2.92	0.78	0.21	13.60
SEGMENT-4	El-Deiba	Erosional	9	1.46	0.48	-0.16	53.16
			10	1.79	0.42	-0.09	85.11
			11	2.21	0.64	0.13	68.73
			12	2.36	0.59	0.18	61.13
			13	1.82	0.46	-0.06	53.81
			14	2.28	0.57	0.16	41.21
SEGMENT-5	El-Gamiel	Depositional	15	2.86	0.67	0.14	18.82
			16	2.26	0.50	0.10	36.12
			17	2.33	0.49	0.09	16.11
			18	2.43	0.59	0.18	12.41

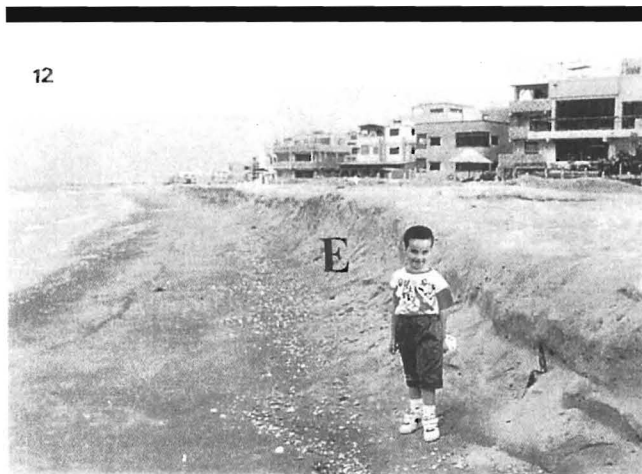


Figure 12. Severe erosion "E" along the sand-nourished beach at El-Gamiel tourist village east of El-Gamiel inlet, with the characteristic steep slope beach face.

other hand, show lower concentrations of total heavy minerals (T.H.M.) range from 0.9% to 19.4% with an average of 7.23% (EL-ASKARY and LOTFY, 1995).

Poor coastal management in the face of the changing sediment transport system along this section of the coast has resulted in a number of problems. El-Gamiel and El-Fardows tourist villages have been constructed at the erosional down-drift east of El-Gamiel inlet. As a result of the pattern of erosion and deposition outlined above, these villages now are suffering erosion (Figures 9 and 12), and need to be protected by construction of detached breakwaters. These defences have encouraged the formation of tombolos (Figure 13), which themselves are interrupting the longshore sediment flux and starving the shoreline down-drift of sediments. Application of a simple coastal GIS (VAN HEUVEL and HILLEN, 1995) using satellite TM images similar to those employed in the present study may facilitate coastal management and would prevent such problems. The recently discovered offshore oil and gas wells at Damietta and Port Said coast may encourage the establishment of oil and gas industry. These ongoing projects may threaten an erosional problem if they constructed in non proper locations.

These results have important implications for the development consequent on the recent discovery of oil and gas reserves offshore. It is important that coastal sediment transport processes are account when any construction is attempted along the Nile Delta coast.

CONCLUSIONS

Remote sensing using Landsat Thematic Mapper (TM) images of the coastline between Damietta and Port Said covering the years 1984, 1987 and 1991 have been used, in association with geomorphological and sedimentological analyses, to determine the pattern of coastal changes in the northeastern Nile Delta. The results enable classifying this section of coast into five segments, on the basis of dominant processes domain and coastline orientation. Segments 1 and

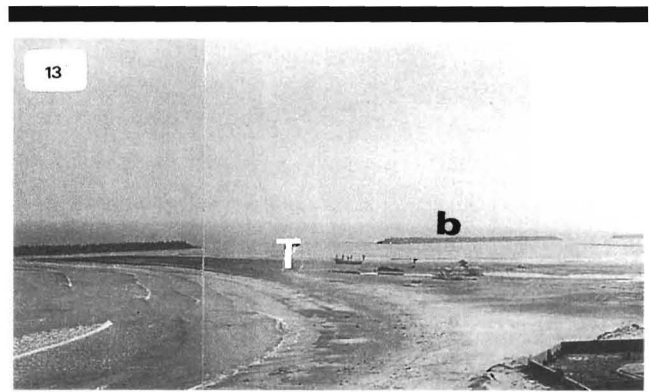


Figure 13. Tombolo "T" formed due to construction of the detached breakwater system "b" to protect the coastline at El-Gamiel tourist village.

2 comprise the coastline east of the mouth of the Damietta branch of the Nile, which experienced significant erosion throughout the study period. Segment-3 comprises the aggrading eastern end of the spit, which has been fed by material eroded from segments 1 and 2 by the eastward-moving longshore flux. Segment-4 comprises El-Deiba, which experienced significant erosion during the period 1984–1987, but was more stable subsequently (1987–1991). Segment-5 comprises the coastline around El-Gamiel. This section of coastline was stable from 1984–1987, even experiencing some accretion in places. However, following construction of an artificial inlet to the Manzala lagoon at some time in the period of 1987–1991, the eastward-moving flux was interrupted by the jetties on either sides of the inlet, resulting in accretion against the western jetty and erosion adjacent to the eastern jetty.

Sediment characteristics of these different shoreline segments show significant differences related to the dominant processes domain operating on each segment. Erosional segments are characterised by relatively coarse sands with high concentrations of heavy minerals, while accretionary segments are characterised by relatively finer sands with lower concentrations of heavy minerals.

Poor coastal management, along with the changes in the sediment transport system outlined in this paper, have created problems by allowing construction to take place along erosional segments of the coast, necessitating costly defence measures. Moreover, these results have important implications for future development consequent on the recent discovery of offshore oil and gas reserves.

ACKNOWLEDGEMENTS

The author would like to express his gratitude to The Royal Society of London, who kindly funded this project. Deep thanks are expressed to Dr. Kevin White, Department of Geography, The University of Reading, U.K. for his continuous help, discussion in the field of Remote Sensing and revision of the manuscript. The contribution of Prof. Paolo A. Pirazzoli is highly appreciated, especially in the final revision of the

manuscript. Finally, the assistance of Ahmed H. El-Asmar during the fieldwork should not be forgotten.

REFERENCES

- ABOU EL-MAGD, I., 1995. Environmental studies on lake Manzala, Egypt using remote sensing and geographic information system. M. Sc. Thesis, El-Mansoura Univ., Egypt.
- BADR, A.A. and LOFFY, M.F., 1998. Measurements of sand transport by spatial method with fluorescent sand tracer along the Damietta promontory, Egypt. *N. Jb. Geol. Paläont. Mh.*, v. 3, p. 129–140.
- BADR, A.A. and LOFFY, M.F., 1999. Tracing beach sand movement using fluorescent quartz along the Nile Delta promontories, Egypt. *Journal of Coastal Research*, v. 15/1, p. 261–265.
- CHEN, P.C. and PAVLIDIS, T., 1979. Segmentation by texture using a co-occurrence matrix and a split-and-merge algorithm. *Computer Graphics and Image Processing*, v. 10, p. 172–182.
- CROSS, A.M.; MASON, D.C., and DURY, S.J., 1988. Segmentation of remotely-sensed images by a split-and-merge process. *Int. J. Remote Sensing*, v. 9, p. 1329–1345.
- EID, F.M.; SHARAF EL-DIN, S.H., and EL-DIN, K.A.A., 1997. Sea level variation along the suz canal, estuarine. *Coastal and shelf sciences*, v. 44, p. 613–619.
- EL-ASKARY, M.A. and LOFFY, M.F., 1995. The use of texture and heavy mineral properties of sand as indicators of the advancing and receding of the Nile Delta beaches, Egypt. *N. Jb. Geol. Paläont. Mh.*, v. 5, p. 257–270.
- EL-ASKARY, M.A. and BADR, A.A., 1996. Foreshore sediments of the Nile Delta promontories: a correlation study. *N. Jb. Geol. Paläont. Mh.*, v. 8, p. 461–472.
- EL-ASMAR, H.M., 1994. Severe coastal damage along Ras El-Bar shoreline, north of the Nile Delta: An effect of the construction of the detached breakwater system. *Journal of Geology, Egypt*, v. 38/2, p. 793–812.
- EL-ASMAR, H.M., 1995. Impact of protection structures on physical and sedimentary parameters along the Damietta coastal area, Nile Delta, Egypt. *Journal of Sedimentology, Egypt*, v. 3, p. 111–124.
- EL-ASMAR, H.M. and WHITE, K., 1997. Rapid updating of maps of dynamic coastal landforms by segmentation of thematic mapper imagery, example from the Nile Delta, Egypt. *Proc. 23rd Ann. RSS Conf.*, The Univ. of Reading, p. 515–520.
- EL-FISHAWI, N., 1994. Relative changes in sea level from tide gauge records at Burullus, central part of the Nile Delta coast. *INQUA MBSS Newsletter*, v. 16, p. 53–61.
- FLECK, M.M., 1992. Some defects in finite-difference edge finders. *IEEE Transactions on Pattern Analysis and Machine Intelligence*, v. 14, p. 337–345.
- FOUCAULT, A. and STANLEY, D.J., 1989. Late Quaternary paleoclimatic oscillations in East Africa recorded by heavy minerals in the Nile Delta. *Nature*, v. 339, p. 44–46.
- FRIEDMAN, G.; SANDERS, J., and KOPASKA-MERKEL, D., 1992. *Principles of sedimentary deposits: stratigraphy and sedimentology*. MacMillan.
- FRIHY, O.E. and KOMAR, P.D., 1993. Long-term shoreline changes and concentration of heavy minerals in beach sands of the Nile Delta, Egypt. *Marine Geology*, v. 115, p. 253–261.
- FRIHY, O.E.; DEWIDAR, KH.M., and EL-BANNA, M.M., 1998a. Natural and human impact on the northeastern Nile Delta coast of Egypt. *Journal of Coastal Research*, v. 14/3, p. 1109–1118.
- FRIHY, O.E.; DEWIDAR, KH.M.; NASR, S.M., and EL-RAFY, M.M., 1998b. Change detection of northwestern Nile Delta of Egypt: shoreline changes, spit evolution, margin changes of Manzala lagoon and its islands. *Int. J. Remote Sensing*, v. 19/10, p. 1901–1912.
- FROUIN, R., SCHWINDLING, M., and DESCHAMPS, P.Y., 1996. Spectral reflectance of sea foam in the visible and near-infrared. *In situ measurements and remote sensing implications. Journal of Geophysical Research*, v. 101/14, p. 361–471.
- HAMAMA, H., 1978. Types and distribution of sediments and landforms in deltaic coastal zone between Ras El-Bar and Port Said. M. Sc. thesis, El-Mansoura Univ., Egypt.
- KETTIG, R.L. and LANDGREBE, D.A., 1976. Classification of multispectral image data by extraction and classification of homogeneous objects. *I.E.E.E. Transactions on Geoscience Electronics*, v. 14, p. 19–26.
- LEMOIGNE, J. and TILTON, J.C., 1995. Refining image segmentation by integration of edge and region data. *I.E.E.E. Transactions on Geoscience and Remote Sensing*, v. 33, p. 605–615.
- LOFFY, M.L., 1978. Geological studies of the coastal zone between Ras El-Bar and Port Said. M. Sc. thesis, Alexandria Univ., Egypt.
- LOFFY, M. and FRIHY, O.E., 1993. Sediment balance in the near-shore zone of the Nile Delta coast, Egypt. *Journal of Coastal Research*, v. 9, p. 654–662.
- MANOHAR, M., 1981. Coastal processes at the Nile Delta coast. *Shore and Beach*, 49, 8–15.
- NAFAA, M.G. and FRIHY, O.E., 1993. Beach and nearshore features along the dissipative coastline of the Nile Delta, Egypt. *Journal of Coastal Research*, v. 9, p. 423–433.
- SESTINI, G., 1989. Nile Delta: a review of depositional environments and geological history. In: WHATELEY, M.K.G. and PICKERING, K.T. (eds) *Deltas: Sites and traps for fossil fuels*, 99–127, Blackwell Scientific Publications, Geol. Soc. London, Special Publ. 41.
- SESTINI, G., 1992. Implication of climatic changes for the Nile Delta. In: JEFFIC, L.; MILLIMAN, J.D., and SESTINI, G. (eds). *Climatic Changes and the Mediterranean*. P. 535–601, Edward Arnold, New York.
- SHARAF EL-DIN, S.H. and MAHAR, A.M., 1997. Evolution of sediment transport along the Nile Delta coast, Egypt. *Journal of Coastal Research*, v. 13/1, p. 23–26.
- SMITH, S.E. and ABDELKADER, A.M., 1988. Coastal erosion along the Nile Delta. *Journal of Coastal Research*, v. 4/2, p. 245–255.
- SONKA, M.; HLAVAC, V., and BOYLE, R., 1993. *Image processing, analysis and machine vision*. Chapman and Hall, London, 555pp.
- STANLEY, D.J. and WINGERATH, J.G., 1996. Nile sediment dispersal altered by Aswan High Dam, the kaolinite trace. *Marine Geology*, v. 133, p. 1–9.
- VAN HEUVEL, T. and HILLEN, R., 1995. Coastline management with GIS in the Netherlands. *EARSEL Advances in Remote Sensing*, v. 4, p. 27–34.
- WESZKA, J.; DYER, C.J., and ROSENFELD, A., 1976. A comparative study of texture measures for terrain classification. *I.E.E.E. Transactions on Systems, Man and Cybernetics*, v. 3, p. 610–621.
- WHITE, K. and EL-ASMAR, H.M., 1999. Monitoring changing position of the coastline using Thematic Mapper Imagery, an example from the Nile Delta. *Geomorphology*, v. 29, p. 93–105.
- WILSON, P.A., 1997. Rule-based classification of water in Landsat MSS images using the variance filter. *Photogrammetric Engineering and Remote Sensing*, v. 63, p. 485–491.